Main Manuscript for

A distinctive neural nexus in blind individuals supports Braille reading.

Ruxue Wang[a,†], Jiangtao Gong[b,c,†], Chenying Zhao[a], Yingqing Xu[b,c,*] and Bo Hong[a,d,*]

[a]Department of Biomedical Engineering, School of Medicine, Tsinghua University, Beijing, 100084, P.R. China;

[b]The Future Laboratory, Tsinghua University, Beijing, 100084, P.R. China;

[c]Academy of Arts & Design, Tsinghua University, Beijing, 100084, P.R. China;

[d]IDG/McGovern Institute for Brain Research, Tsinghua University, Beijing, 100084, P.R. China

[†]R.W. and J. G. contributed equally to this work.

*Correspondence should be addressed to Bo Hong or to Yingqing Xu.

Email: hongbo@tsinghua.edu.cn; yqxu@tsinghua.edu.cn

Author Contributions: B.H., Y.X., R.W. and J.G. designed the research; R.W. and J.G. performed the research; R.W., J.G. and C.Z. collected the data; R.W. and J.G. analysed the data; R.W., B.H., J.G. and Y.X. wrote and improved the paper.

Competing Interest Statement: The authors declare no competing financial interests.

Keywords: natural Braille reading | acquired blindness | ‘visual’ cortex | crossmodal plasticity | top-down modulation

Abstract

In the absence of visual input, occipital 'visual' cortex of blind people has been found to be engaged in non-visual higher cognitive tasks. Although the increased functional connectivity between 'visual' cortex and frontal cortex in the blind has been observed, the specific organization and functional role of this connectivity change remain to be elucidated. Here, we tested resting-state functional connectivity for primary 'visual' cortex (V1) and higher-tier lateral occipital cortex (LOC) in people with acquired blindness, and found an enhanced connectivity between the LOC but not V1 and typical frontal language areas - the inferior frontal cortex (IFC). In fact, the left-lateralized LOC-IFC connectivity strength predicted blind individuals' natural Braille reading proficiency. Furthermore, an increased bidirectional information flow between the left LOC and IFC was observed during a natural Braille reading task. In particular, the task-relevant modulation of the top-down communication from left IFC to LOC was significantly stronger than that of the bottom-up communication. Altogether, our study identified a distinctive neural nexus, LOC-IFC connection, and its behavioral significance in the acquired blind, revealing the neural correlates of the crossmodal plasticity in their 'visual' cortex underlying natural Braille reading.

Main Text

Introduction

Tactile Braille reading is a demanding skill that allows blind humans to achieve literacy (1, 2). It involves many systems beyond the somatosensory system for processing tactile input, including the recruitment of the visual cortex and higher-order language systems (3–6). While there are several studies on the neural correlates of Braille reading, most of these studies employed either only Braille letter (7–9) or Braille word (1, 4, 6, 10–13) recognition rather than the natural Braille reading of complete sentences. Therefore, the neural basis of natural Braille reading, including the interaction of the visual system and genuine language systems, is not yet fully understood. It has been shown that Braille words significantly activate an extended area of the 'visual' cortex stretching from the primary 'visual' cortex (V1) to higher-tier 'visual' regions—the lateral occipital cortex (LOC) in blind humans (14, 15), including peak activation in the approximately consistent area as the typical visual word form area (VWFA) in sighted individuals (6, 11, 15).

Moreover, functional connectivity patterns between the 'visual' cortex and other areas of the brain have been found to be altered in blind humans. One of the most robustly found changes in connectivity is that between the 'visual' cortex and frontal cortex (16–18). However, it remains a matter of debate which specific region within the occipital cortex entertains stronger functional connectivity with frontal language areas (19–23). Some studies have reported that V1 has increased functional connectivity with language areas—the inferior frontal cortex (IFC) (19, 20)—in blind individuals relative to sighted controls, while others found that instead of V1, the LOC in blind humans exhibits an enhanced connectivity with the IFC (21–23). We

hypothesized that the LOC in blind individuals may act as the multisensory integration area, bridging Braille shape recognition and language-related components of Braille reading and that the functional connectivity between the LOC and IFC might support the Braille reading behavior of blind individuals.

In addition, why the 'visual' cortex is more actively engaged in various crossmodal tasks in blind humans, including late blind humans, than in sighted controls is still debated (24). Here, we use Braille reading as a model to investigate the hypothesis that 'visual' cortex activity in late blindness predominantly arises from the top-down connectivity from higher-order multisensory or supramodal cortex (24, 25). Many researchers have been concerned about the direction of the functional connectivity between the 'visual' and higher-order frontal areas of blind individuals (22, 26, 27). Some researchers have proposed that there might be bidirectional information transmission between these two areas for further processing (26). Other researchers have stressed the predominant role of top-down connectivity, e.g., from the frontal cortex, which mediates the activity of the 'visual' cortex in higher-cognitive tasks in blind humans (22, 27). However, studies investigating the direction of the 'visual'-IFC functional connectivity are lacking. The present study directly addressed this open question by examining the dynamic communication between the 'visual' cortex and language frontal areas in blind humans during natural Braille reading.

This study focused on Braille readers with acquired blindness. To fully investigate the behavior and neural correlates of natural Braille reading, as shown in Fig. 1, we first assessed the blind subjects' Braille reading proficiency with natural Braille articles and recorded their self-reported amount of Braille reading practice time for different age periods. We quantified the resting-state functional connectivity with frontal language areas for two visual brain regions, V1 and LOC, in blind humans to determine whether this connectivity could predict the Braille reading performance of blind individuals. Furthermore, we asked these blind subjects to perform a natural Braille reading task during functional magnetic resonance imaging (fMRI) acquisition and employed dynamic causal modelling (DCM) to investigate the direction of information flow between the visual and frontal language areas in blind humans.

Results

Heightened functional connectivity for the higher-tier 'visual' cortex in the blind group. Taking the sighted group as the reference, we tested functional connectivity changes in the blind group for two visual brain regions, V1 and LOC, for the two hemispheres separately. The functional connectivity for V1 was not different between the blind and sighted groups. In both groups, we found significant connections of V1 with other visual areas but not with frontal language areas—the IFC (Fig. 2A). By contrast, we observed significantly stronger functional connectivity of the LOC with the IFC in the blind group than in the sighted group (Fig. 2B, C). Unsurprisingly, prominent connections of the LOC with other visual regions and extensively with dorsal parietal regions were found in both groups.

In addition, despite significant connections between the LOC seed and IFC in both hemispheres in the blind group (vertexwise $P < 10^{-6}$, uncorrected, cluster size > 100 mm), the functional connections of the bilateral LOC with only the left IFC but not the right IFC in the blind group were significantly stronger than those in the sighted controls (Fig. 2C, $P < 0.025$, permutation test with threshold-free cluster enhancement correction for each hemisphere, cluster size > 15 mm). In addition, we also found significantly stronger functional connectivity between the left LOC and left intraparietal sulcus (IPS) in the blind group than in the sighted group (Fig. 2C left panel, Supplementary Figure 1).

Left LOC-IFC functional coupling predicts Braille reading behavior in blind individuals. To test our hypothesis that the reorganized functional connectivity for the LOC is relevant to Braille reading behavior, we examined whether this functional connectivity predicted individual levels of Braille reading proficiency and whether there was an additional correlation with the amount of Braille reading practice time. We performed an additional Braille reading behavioral test to estimate the Braille reading proficiency of our blind participants using natural Braille articles. The behavioral tests showed that blind individuals had various levels of Braille reading proficiency, with an average reading speed of 107.52 ± 50.45 (mean ± s.d.) Braille words per minute, and an average accuracy of 99.84 ± 0.17% (mean ± s.d.). We found that a stronger left LOC-IFC functional connectivity contributed to a higher Braille reading proficiency (Spearman correlation, n = 14, $P = 0.013$, $r = 0.644$; Pearson correlation, n = 14, $P = 0.159$, $r = 0.397$). This relation survived after controlling for the age of blindness onset, age and mean framewise displacement (28) (motion) in the resting-state scan (Fig. 3A left panel, partial Spearman correlation, $P = 0.026$, $r = 0.665$; partial Pearson correlation, $P = 0.358$, $r = 0.308$). By contrast, the right LOC-left IFC functional connectivity was not correlated with the blind individual's Braille reading proficiency (Fig. 3B left panel, partial Spearman correlation, $P = 0.180$, $r = 0.436$; partial Pearson correlation, $P = 0.358$, $r = 0.307$). There was no significant correlation between left V1-IFC connectivity and Braille reading proficiency in the blind group (Supplementary Table 1). In addition, although the connectivity strength of the left LOC-IPS in the blind group was enhanced (Supplementary Figure 1), this functional connectivity did not predict individual Braille reading proficiency (Supplementary Table 1).

Blind participants were further asked to answer a detailed questionnaire on the self-estimated amount of Braille reading practice time for different age periods, including childhood, adolescence, and adulthood. We then calculated the correlations between the functional connectivity for the LOC and individual Braille practice time in each age period respectively. Braille reading practice time (in hours) during adolescence was significantly and positively correlated with the left LOC-IFC functional connectivity in blind individuals (Pearson correlation, n = 14, $P = 0.003$, $r = 0.724$; Spearman correlation, n = 14, $P = 0.029$, $r = 0.582$). This correlation still reached significance after controlling for the age of blindness onset, age and head motion (28) in the scan (Fig. 3A right panel, partial Pearson correlation, $P = 0.013$, $r = 0.718$; partial Spearman correlation, $P = 0.052$, $r = 0.598$). Additionally, the total Braille reading practice time (in hours) was significantly and positively correlated with the left LOC-IFC connectivity (Pearson correlation, n = 14, $P = 0.032$, $r = 0.574$; Spearman correlation, n = 14, $P = 0.072$, $r = 0.495$). It was also nearly significant for the partial correlation

(Supplementary Figure 2A). Neither Braille reading practice time during childhood nor during adulthood showed a significant correlation with this functional connectivity (Supplementary Figure 2A). By contrast, the right LOC-left IFC functional connectivity was not significantly correlated with blind people's Braille reading practice time (in adolescence, Fig. 3B right panel, partial Pearson correlation, $P = 0.513$, $r = 0.221$; partial Spearman correlation, $P = 0.322$, $r = 0.330$; in other age periods, Supplementary Figure 2B). Similarly, the left V1-IFC connectivity and the increased left LOC-IPS connectivity did not correlate with blind individuals' Braille reading practice time (Supplementary Table 1).

In summary, although there was a significant increase in both the left LOC-left IFC and the right LOC-left IFC functional connectivities, only the left-lateralized LOC-IFC functional connectivity was significantly associated with Braille reading behaviors. The left LOC-IFC functional coupling predicted an individuals' Braille reading proficiency and Braille reading practice time.

Bidirectional left LOC-IFC information flow for Braille reading with asymmetrically stronger top-down modulation. Next, we employed dynamic causal modelling (DCM) to assess the direction of the LOC-IFC effective connectivity during Braille reading and investigated how this connectivity was modulated by the task. The blind subjects were asked to silently read pages containing natural Braille articles while undergoing fMRI, with no-Braille blank pages as the control. The Braille > blank contrast elicited activations in the bilateral V1, LOC, IPS and left IFC in blind subjects (Supplementary Figure 3). In addition, we constrained our DCM models to the left hemisphere due to the left-lateralized activation of the IFC and the left-lateralized increased LOC-IFC and LOC-IPS functional connections in the blind individuals. Therefore, four brain regions, IPS, V1, LOC, and IFC—which are all frequently implicated in Braille reading (2, 4)—were selected for further DCM analysis.

We specified the model space as shown in Fig. 4A. The null model represents the basic structure, including endogenous effective connectivity among ROIs and the modulation of the IPS-LOC connection confirmed in previous studies (8). Considering the consistent finding that tactile information from the somatosensory cortex was redirected to the occipital cortex through the poly-sensory intraparietal cortex (2, 8, 29), we used the IPS to model the tactile input for the LOC. To investigate the dynamic interactions between the left LOC and the left IFC in the blind individuals, each direction of this connection can be either modulated or not, thus obtaining four possible models. Individual fixed-effects Bayesian model selection (BMS) showed that the bidirectional modulation model fit the data of most blind individuals best, except for one blind subject, for whom the top-down model was selected. Further application of random-effects Bayesian model selection (BMS) at the group level showed that the bidirectional model clearly outperformed the other three models (Fig. 4B, exceedance probability [the probability that a particular model is more likely than any other model] = 51.24%).

Bayesian model averaging (BMA) was applied to the winning model (Supplementary Tables 2, 3) and showed that the endogenous connectivity and modulatory effect parameters

between the LOC and IFC were all significant (Fig. 4C, posterior probabilities > 0.99). As illustrated in Figure 4c, the LOC-to-IFC endogenous connectivity was positive (0.190 s^{-1}), while the IFC-to-LOC connectivity was negative (-0.491 s^{-1}), indicating that irrespective of the task-relevant modulation, the activity changes in the LOC increased the activity in the IFC but not vice versa. The modulation effects of Braille reading on the left LOC-IFC bidirectional connections were both positive in the blind group, with a modulation strength of + 0.362 s^{-1} for the bottom-up connection and + 0.692 s^{-1} for the top-down connection (Fig. 4C left panel). Notably, the Braille reading task-relevant modulation of the top-down communication from the left IFC to the LOC was significantly stronger than that of the bottom-up communication, from the LOC to the IFC (Fig. 4C, $P < 0.001$). This asymmetrical modulation highlights the functional relevance to natural Braille reading of the top-down communication from the left IFC to the left LOC in blind individuals.

Discussion

In this study, we collected natural Braille reading behavior data and resting-state and task fMRI data from 14 subjects with acquired blindness, to investigate the neural correlates of crossmodal plasticity in the 'visual' cortex underlying Braille reading. We observed that the left higher-tier 'visual' cortex LOC rather than the primary 'visual' cortex V1 entertained stronger functional connectivity with frontal language area IFC in late blind humans. Importantly, we further showed that the left-lateralized LOC-IFC functional connectivity was positively correlated with the Braille reading practice time of blind individuals, especially in adolescence. Furthermore, a stronger left LOC-IFC connectivity predicted better natural Braille reading proficiency. In addition, in a natural Braille reading task, bidirectional left LOC-IFC information flow for Braille reading with asymmetrically stronger task-relevant top-down modulation emerged in the DCM model. Altogether, our findings concur in suggesting that the enhanced functional connectivity between the left LOC and the left IFC in acquired blindness serves as a key neural nexus that bridges tactile Braille recognition and higher-level language processing in natural Braille reading.

The crossmodal recruitment of the typical visual cortex for nonvisual functions in blind humans has been frequently observed (24, 27, 30–33). However, one matter of debate surrounding this dramatic plasticity is whether there is a reversed hierarchy of functional organization across 'visual' areas or not (10, 14, 21, 34). A study of congenitally blind individuals showed a preference for more 'abstract' aspects (verbal memory) in early V1, while higher-tier visual areas processed more 'sensory' aspects, suggesting a reversal of the normal hierarchy in the visual systems of sighted individuals (10, 34). This is supported by findings of increased long-range connectivity between V1 and the higher-order frontal cortex in blind humans (19, 20). Some studies reported activations of both the primary and higher-level 'visual' regions in early and late blind subjects during language-related tasks (4, 22, 35, 36). Other studies, however, did not support the reversed pattern of organization by specifically identifying the role of the higher-tier 'visual' cortex in cognitive tasks and its functional connectivity with frontal language areas in individuals with early blindness and

anophthalmia (21, 23). The current study showed that late blind individuals had developed increased left LOC-IFC functional connectivity that was positively correlated with their Braille reading performance, instead of the V1-IFC connectivity, which suggested a normal functional hierarchy in 'visual' regions of late blind humans. This is not implausible since late blind individuals might have initially developed their neural circuits as a normal sighted person (24). Note that this study employed an anatomically defined higher-tier 'visual' cortex, the LOC, in late blind humans, approximately encompassing the location of the visual word form area (VWFA) in sighted people. The typical VWFA in sighted is a reading-specific area that is tuned to orthographic word structure not only in visual word reading (37, 38) but also in tactile reading after Braille training (9, 12, 13). In tactile Braille reading, similar responses have been found in the 'VWFA' in blind humans to those in the VWFA in sighted humans (15, 27). It was suggested that the higher-tier 'visual' cortex served as a particularly important entry node for tactile signals (2) and extracted abstract Braille shape information for further linguistic-related processing in frontal regions (2). Additionally, some other studies have reported a less reading-specialized 'VWFA' in blind individuals and that its activations in some functions, possibly for example, general language processing (6, 11, 15), are similar to those in the higher-tier 'visual' cortex, the LOC (21–23, 27). With the brain-behavior evidence in this study, we thus assume that the left LOC in late blind humans becomes a more extensive and versatile crossmodal region incorporating a VWFA-like function that bridges tactile Braille orthographic and language processing in Braille reading, resulting in a distinctive neural nexus of the left LOC-IFC. The development of this connectivity might be based on the existing crossmodal connectivity between the left VWFA and the genuine language area, the IFC, in sighted individuals (39–41). This prominent brain rewiring in late blind people also provides new evidence for the "connectivity-based" plasticity theory (27, 42, 43).

How does the observed crossmodal plasticity of the LOC in late blind humans emerge? With DCM analysis, we directly addressed this question by revealing the direction of the information flow on the distinctive neural connection between the left LOC and the higher-order language area, left IFC, during a natural Braille reading task. The winning bidirectional model for the blind subjects (Fig. 4A, B) is in line with the Hebbian theory (44) that the constant information flow between the left LOC and IFC during Braille reading might strengthen such crossmodal connection. Our results thus extend the behavioral principle that "practice makes perfect" by showing positive correlations between this strengthened connectivity in the resting state and both Braille reading practice time and proficiency. In particular, the asymmetrically stronger task-relevant top-down modulation of the left IFC-to-LOC connection during Braille reading (Fig. 4C) provides important evidence for the top-down controlled learning mechanism in late blind humans (24); that is, the crossmodal capacities of the genuine visual cortex in late blind individuals are possibly mediated by feedback connections from higher-order neural systems tuned during task-relevant learning (24). This is likely essential for late blind individuals because their visual deprivation onset occurs after the pruning of exuberant crossmodal connectivity during the early phases of typical development (24, 44); therefore, it might be relatively difficult for them to extract crossmodal characteristics exclusively via bottom-up, stimulus-driven input (24, 45). Our finding of the task-specific top-down influence on left LOC activity is in accord with a study that showed stronger task-

induced ‘visual’ cortex activity in individuals with acquired blindness due to active task interpretation (47) as well. This top-down mediated plasticity in late blind humans is compatible with the typical adult neural learning mechanisms demonstrated by several human and non-human animal studies (24, 46, 48, 49). Additionally, as suggested by researchers (24, 45, 50) that the elaboration of feedback connectivity might require stimulus-driven input, our results further implied that in Braille reading, the bottom-up left LOC-IFC effective connectivity provided Braille shape information input to the IFC; thus, the genuine language area, left IFC, predicted the pattern of activity within the ‘visual’ area, left LOC, based on the prior association of tactile Braille characteristics with semantic and conceptual knowledge (51) and then delivered top-down modulation to the LOC. This is also in line with the predictive coding framework (52, 53). Altogether, the present study suggests that the activity of the left LOC in late blind humans does not exclusively arise from sensory input but is predominantly driven by task-relevant top-down information flow from the IFC.

Different from other studies using Braille letters or words, the large-scale Braille articles used in our study made it possible to observe task-relevant top-down communication in blind humans during natural Braille reading. We thus speculate that a promising strategy for blind Braille readers to make better use of this top-down connectivity during natural Braille reading might be to make the context more available. Compared with traditional refreshable Braille displays offering only a single-line of characters (54), an emerging technology is the large-print Braille computer (55, 56), which displays continuous and large-scale natural Braille contexts. This new type of Braille reading device likely allows for active understanding and prediction based on contextual information during natural Braille reading and may accelerate the purposeful brain rewiring of late blind people.

Materials and Methods

Subjects. 14 blind (7 males) and 15 sighted subjects (8 males) participated in the study. All subjects were right handed and had no history of neurological disorder. Participants in the blind group were undergraduate students studying at a special education college (mean age ± s.d. = 21.92 ± 1.97 years) and were all Braille readers with acquired blindness (Table 1). Sighted subjects had normal or corrected-to-normal vision and had never learned Braille. One sighted subject with excessive head motion (mean framewise displacement [FD (28); > 2 SD from the group mean]) during fMRI acquisition was excluded from further analyses, leaving 14 sighted subjects (7 males, mean age ± s.d. = 21.73 ± 1.07 years). The two groups were matched in age (two sample *T*-test, n = 14 in the blind group and n = 14 in the sighted group, *T*-value = 0.325, CI [-1.054 1.443], DF = 26, *P* = 0.748, Cohen’s *d* = 0.123, two-tailed). The study was approved by the Institutional Review Board of Tsinghua University, and informed consent was obtained from each of the participants.

Acquisition of biographical data on Braille reading practices. Each blind subject was asked to answer a detailed questionnaire on the self-estimated amount of time (in hours) spent in Braille reading practice during different age periods (16). The subjects were asked to

retrospectively identify key events in their Braille practice, such as when they started to learn Braille reading and when they changed the amount of time for Braille reading practice. They thereafter estimated the average hours of Braille reading practice per week in the time periods between these key events. We then calculated the total time of Braille reading practice during three different age periods: childhood (from the start of Braille reading to the age of 11 years), adolescence (12–16 years) and adulthood (from the age of 17 years to the exact time of the experiment). See Table 1 for details of the Braille reading practice of the blind subjects.

Braille reading performance test. The blind subjects were asked to participate in a Braille reading behavioral test resembling real-life reading prior to fMRI acquisition to estimate their Braille reading proficiency. See SI materials and methods for further details.

The task was to read the 2 natural Braille articles aloud as accurately and quickly as possible. The reading strategy was not specified. We measured the number of Braille words correctly read per minute on average for each blind subject. If a word was read inaccurately, it was not counted in the final Braille proficiency score. Individual Braille reading accuracies were also assessed by calculating the proportion of Braille words correctly read to the total words in the 2 Braille articles. To avoid situations in which the difficulty in Braille reading comprehension was because of one's unfamiliarity with individual Braille words, blind individuals with a reading accuracy exceeding a threshold of 99.5% were recruited in this study.

Functional MRI parameters. All MR images were acquired from a Philip Achieva 3.0 Tesla TX MR scanner with a 32-channel head coil. All subjects were asked to keep their eyes closed during the scans. See SI materials and methods for further details.

Resting-state fMRI data preprocessing and analysis. Structural data were processed and reconstructed to individual cortical surface using FreeSurfer. Individual resting-state data were preprocessed using the following procedures: (i) discarding of the first 4 volumes; (ii) slice-timing correction; (iii) rigid body correction for head motion with the AFNI package (57); (iv) functional-anatomical image co-registration; (v) bandpass temporal filtering (0.01-0.08 Hz); and (vi) regressing out of nuisance covariates to control for physiological effects and head motion (6 head motion parameters and 2 regressors corresponding to the ventricular signal and white matter signal). The preprocessed fMRI data of each subject were first aligned to the reconstructed individual cortical surface in each hemisphere. Then, a 6-mm full-width half-maximum (FWHM) Gaussian smoothing kernel was applied to the fMRI data in the surface space. The smoothed data were then down-sampled to the FreeSurfer template with 2,562 vertices in each hemisphere using the mri_surf2surf function in FreeSurfer. To ensure reliable measures of functional connectivity, we combined the fMRI data of two resting-state scans for further analyses.

The primary visual cortex (V1) was defined as the combination of the occipital pole and calcarine sulcus in FreeSurfer's automatic anatomical parcellation (aparc2009) (58), consistent with the location of V1 in previous studies (19, 21, 22). In agreement with the seed

regions in prior functional connectivity analyses of blind and sighted individuals (21, 22, 59), we used the lateral occipital cortex as a higher-tier visual seed, located in the anatomical occipital areas in FreeSurfer aparc2009 atlas (58) (combining the middle occipital gyrus and sulcus, anterior occipital sulcus, inferior occipital gyrus and sulcus, and lateral occipital-temporal sulcus). The V1 and LOC regions were used as the seeds for functional connectivity (FC) analyses.

To obtain the whole-brain functional connectivity patterns of each seed region, we computed the correlation between the mean blood oxygen level-dependent (BOLD) signal of the seed region and the time series of every other vertex in both hemispheres for each subject. These r-maps were next converted into z-maps using Fisher's r-to-z transformation. All statistical group-level FC pattern analyses were carried out using the Surface-Based Data Processing & Analysis for (Resting-State) Brain Imaging software (DPABISurf 1.1) (60). A one-sample *T*-test (n = 14 in the blind group and n = 14 in the sighted group, DF = 13 for each group respectively, one-tailed) was performed for individual FC z-maps to generate significant and positive FC maps (vertexwise $P < 10^{-6}$, uncorrected, cluster size > 100 mm) of the V1 or LOC region for each group. Thus, a union mask including identified significant vertices in either the blind or sighted group was created for further FC pattern comparison between the two groups (61). Recent works have consistently suggested that the influence of head motion on intrinsic functional connectivity in the analysis of between-group functional connectivity comparison needs to be further scrutinized regardless of the correction one employs at the individual level (28, 62). We therefore calculated the mean framewise displacement (FD) (28), describing the mean absolute displacement of each brain volume relative to the previous volume in translation and rotation in the x, y, and z directions during the resting-state scan for each subject.

With mean FD as the covariate controlling for the head motion effect (61), we conducted a two-sample *T*-test (n = 14 in blind group and n = 14 in sighted group, DF = 26, two-tailed) on the basis of individual FC z-maps within the union mask to examine how the V1 or LOC FC patterns of the blind group changed with respect to the sighted group, and the significant vertices were those surviving the multiple comparison correction using non-parametric permutation testing (63) (5,000 permutations) and threshold-free cluster enhancement (64) ($P < 0.025$, corrected for each hemisphere, cluster size > 15 mm).

Statistical analysis on the relationship between functional connectivity and behavioral data. We further tested for a relationship between enhanced functional connectivity and Braille reading behavioral data in blind individuals. Considering that the overall whole-brain connection strength varies among individuals, we z-normalized the functional connectivity for each subject. We next calculated the Pearson correlation and Spearman correlation coefficients between individuals' normalized 'visual'-related functional connectivity and, separately, their Braille reading proficiency, Braille reading practice time within different age periods and total Braille reading practice time. Moreover, we tested partial correlations among these parameters with covariates of the onset age of blindness, the age when the blind

individuals participated in the experiment and motion in the resting state scan indexed by mean FD (65).

FMRI task paradigm. A natural Braille reading task with 10 blocks was used in this study (Supplementary Figure 3). See SI materials and methods for further details.

Task fMRI Data preprocessing and analysis. The task fMRI data were preprocessed using the FsFast software package (http://surfer.nmr.mgh.harvard.edu/fswiki/FsFast). The preprocessing procedures first included motion correction, slice timing correction, and boundary-based functional-anatomical alignment. Similar to the resting-state fMRI, the task fMRI data of each subject were registered to the reconstructed individual cortical surface. The fMRI data were smoothed with a Gaussian filter (FWHM = 6 mm) in the surface space. The smoothed data were then down-sampled to the FreeSurfer template with 2,562 vertices in each hemisphere. One blind subject (B7) who presented with excessive head motion (mean FD (28); > 2 SD from the group mean) during the Braille reading task fMRI scan was excluded from further GLM and DCM analyses, leaving 13 blind subjects (7 males).

Functional MRI analyses were carried out using Statistical Parametric Mapping toolbox (SPM12, Welcome Department of Imaging Neuroscience, Institute of Neurology, London). For the first-level individual analysis, functional images were modelled with 3 regressors (one for the Braille condition, one for the blank condition, and another for the turning page condition, which was discarded in the analysis) using the general linear model (GLM) method. Head motion regression was also performed in the analysis. We defined a Braille > blank contrast to reveal activated brain regions (significant $P < 0.025$ for each hemisphere, uncorrected). We did not set an extremely strict threshold here because the aim of these GLM analyses was to yield brain regions showing task-relevant effects for further DCM analyses. For group-level GLM analysis, all the blind group subjects' data were concatenated and then analysed by a one-sample *T*-test (n = 13 in the blind group, DF = 12, one-tailed). Significant brain activations in the blind group were also revealed by the Braille > blank contrast (Supplementary Figure 3, significant $P < 0.025$ for each hemisphere, uncorrected).

Dynamic causal modelling (DCM). All DCM analyses were carried out using SPM12. DCM is a computational framework for explaining the effective connectivity and interactions among brain regions that show experimental effects (66). Posterior probability analysis in DCM determines the most likely coupling parameters at the neuronal level given the measured BOLD signals according to the specified model and priors on the coupling and haemodynamic parameters. In our case, we focused on the dynamic interactions among the IPS, LOC, V1 and IFC in the left hemisphere that were activated when the blind subjects were reading the natural Braille articles. The very exact left V1, LOC and IFC areas in the resting-state analysis and the larger anatomical region of the IPS (intraparietal sulcus, defined in the FreeSurfer aparc2009 atlas (58)) were used as anatomical masks for defining regions of interests (ROIs) later. Each subject-specific ROI consisted of all significant vertices revealed by the Braille > blank contrast exceeding a threshold of $P < 0.025$ for each hemisphere (uncorrected, cluster size > 5 vertices) within the corresponding anatomical mask. The time series of these ROIs

were then extracted for each subject. We did not set the threshold of cluster size for one blind subject who lacked a strong response in one ROI to ensure that significant vertices could be identified from each of the 4 ROIs (67).

Typically, there are 3 types of DCM parameters (66): 1) endogenous parameters, reflecting the task-independent effective connectivity among regions; 2) driving effects, which quantify how neural responses change due to the task stimuli; and 3) modulatory strengths, the parameters of greatest interest, which account for the changes in specific effective connectivity due to the task-relevant conditions. Bidirectional endogenous connections among the 4 ROIs were constructed based on anatomical knowledge and our resting-state functional connectivity results. We used the IPS to model the tactile input for the LOC, consistent with the finding that tactile information from the somatosensory cortex was redirected to the 'visual' systems through the poly-sensory intraparietal cortex in blind people (2, 8, 29). We set the modulatory effect of Braille reading on the connectivity between the left IPS and LOC in accord with a prior study (8). We then investigated the task-specific modulatory effect of Braille reading on the connection between the left LOC and IFC. Therefore, we considered that the task-relevant information flow on any direction (bottom-up and top-down) between these two regions might be modulated, resulting in 4 competing models (Fig. 4A).

We first performed Bayesian model selection (BMS) with fixed-effects analysis to select the winning model for each subject and then performed BMS with random-effects analysis to select the winning model at the group level after balancing the explanation of data and the model complexity. The exceedance probability intuitively presented the relative preference within all models (Fig. 4B). To make inferences on the group-level model parameters, Bayesian model averaging (BMA) was then employed on the winning model. BMA can estimate the full posterior density on parameters (68). Therefore, the significance of each connectivity parameter could be assessed by the fraction of samples in the posterior density (out of 10,000 sampled data points) that were different from zero (69). The significance of the difference in modulatory strengths on one connection versus another connection was assessed by the fraction of samples that were higher for one connection than another (69).

Acknowledgments

This work is supported by the National Science Foundation of China [grant number NSFC 61621136008] and National Key R&D Program of China [grant number 2017YFA0205904 B.H.]. We thank Brigitte Röder at the University of Hamburg for comments on the manuscript.

References

1. N. Sadato, et al., Neural networks for Braille reading by the blind. Brain 121, 1213–1229 (1998).

2. N. Sadato, How the blind “see” Braille: Lessons from functional magnetic resonance imaging. Neuroscientist 11, 577–582 (2005).
3. R. Hamilton, J. P. Keenan, M. Catala, A. Pascual-Leone, Alexia for Braille following bilateral occipital stroke in an early blind woman. NeuroReport 11, 237–240 (2000).
4. H. Burton, et al., Adaptive Changes in Early and Late Blind: A fMRI Study of Braille Reading. Journal of Neurophysiology 87, 589–607 (2002).
5. A. Pascual-Leone, A. Amedi, F. Fregni, L. B. Merabet, the Plastic Human Brain Cortex. Annual Review of Neuroscience 28, 377–401 (2005).
6. Katarzyna Rączy, et al., Orthographic Priming in Braille Reading as Evidence for Task-specific Reorganization in the Ventral Visual Cortex of the Congenitally Blind. Journal of Cognitive Neuroscience 31, 1065–1078 (2019).
7. L. G. Cohen, et al., Functional relevance of cross-modal plasticity in blind humans. Nature 389, 180–183 (1997).
8. T. Fujii, H. C. Tanabe, T. Kochiyama, N. Sadato, An investigation of cross-modal plasticity of effective connectivity in the blind by dynamic causal modeling of functional MRI data. Neuroscience Research 65, 175–186 (2009).
9. Ł. Bola, et al., Functional hierarchy for tactile processing in the visual cortex of sighted adults. NeuroImage 202 (2019).
10. A. Amedi, N. Raz, P. Pianka, R. Malach, E. Zohary, Early “visual” cortex activation correlates with superior verbal memory performance in the blind. Nature Neuroscience 6, 758–766 (2003).
11. J. S. Kim, S. Kanjlia, L. B. Merabet, M. Bedny, Development of the Visual Word Form Area Requires Visual Experience: Evidence from Blind Braille Readers. The Journal of Neuroscience 37, 11495–11504 (2017).
12. J. Matuszewski, et al., Brain plasticity dynamics during tactile Braille learning in sighted subjects: Multi-contrast MRI approach. NeuroImage 227, 117613 (2021).
13. K. Siuda-Krzywicka, et al., Massive cortical reorganization in sighted braille readers. eLife 5, 1–26 (2016).
14. H. Burton, Visual cortex activity in early and late blind people. Journal of Neuroscience 23, 4005–4011 (2003).
15. L. Reich, M. Szwed, L. Cohen, A. Amedi, A ventral visual stream reading center independent of visual experience. Current Biology 21, 363–368 (2011).
16. Y. Liu, et al., Whole brain functional connectivity in the early blind. Brain 130, 2085–2096 (2007).
17. D. Wang, et al., Altered resting-state network connectivity in congenital blind. Human Brain Mapping 35, 2573–2581 (2014).
18. N. Sabbah, et al., Increased functional connectivity between language and visually deprived areas in late and partial blindness. NeuroImage 136, 162–173 (2016).
19. O. H. Butt, N. C. Benson, R. Datta, G. K. Aguirre, The fine-scale functional correlation of striate cortex in sighted and blind people. Journal of Neuroscience 33, 16209–16219 (2013).
20. E. Striem-Amit, et al., Functional connectivity of visual cortex in the blind follows retinotopic organization principles. Brain 138, 1679–1695 (2015).

21. K. E. Watkins, et al., Language networks in anophthalmia: Maintained hierarchy of processing in “visual” cortex. Brain 135, 1566–1577 (2012).
22. M. Bedny, A. Pascual-Leone, D. Dodell-Feder, E. Fedorenko, R. Saxe, Language processing in the occipital cortex of congenitally blind adults. Proceedings of the National Academy of Sciences (2011) https:/doi.org/10.1073/pnas.1014818108.
23. U. Noppeney, Effects of visual deprivation on the organization of the semantic system. Brain 126, 1620–1627 (2003).
24. B. Röder, R. Kekunnaya, M. J. S. Guerreiro, Neural mechanisms of visual sensitive periods in humans. Neuroscience and Biobehavioral Reviews 120, 86–99 (2021).
25. O. Collignon, et al., Impact of blindness onset on the functional organization and the connectivity of the occipital cortex. Brain 136, 2769–2783 (2013).
26. B. Deen, R. Saxe, M. Bedny, Occipital Cortex of Blind Individuals Is Functionally Coupled with Executive Control Areas of Frontal Cortex. Journal of Cognitive Neuroscience 27, 1633–1647 (2015).
27. M. Bedny, Evidence from Blindness for a Cognitively Pluripotent Cortex. Trends in Cognitive Sciences 21, 637–648 (2017).
28. J. D. Power, K. A. Barnes, A. Z. Snyder, B. L. Schlaggar, S. E. Petersen, Spurious but systematic correlations in functional connectivity MRI networks arise from subject motion. NeuroImage 59, 2142–2154 (2012).
29. G. F. Wittenberg, K. J. Werhahn, E. M. Wassermann, P. Herscovitch, L. G. Cohen, Functional connectivity between somatosensory and visual cortex in early blind humans. European Journal of Neuroscience 20, 1923–1927 (2004).
30. B. Röder, H. J. Neville, “Developmental plasticity” in Handbook of Neuropsychology, J. Grafman, I. Robertson, Eds. (Elsevier, 2003), pp. 231-270.
31. L. Renier, A. G. De Volder, J. P. Rauschecker, Cortical plasticity and preserved function in early blindness. Neuroscience and Biobehavioral Reviews 41, 53–63 (2014).
32. B. Heimler, A. Amedi, Are critical periods reversible in the adult brain? Insights on cortical specializations based on sensory deprivation studies. Neuroscience and Biobehavioral Reviews 116, 494–507 (2020).
33. F. Pavani, B. Röder, “Crossmodal plasticity as a consequence of sensory loss: Insights from blindness and deafness” in The New Handbook of Multisensory Processes., B. E. Stein, Ed. (Cambridge, MA: MIT Press, 2012), pp. 737–760.
34. C. Büchel, Cortical hierarchy turned on its head. Nature Neuroscience 6, 657–658 (2003).
35. B. Röder, O. Stock, S. Bien, H. Neville, F. Rösler, Speech processing activates visual cortex in congenitally blind humans. European Journal of Neuroscience (2002) https:/doi.org/10.1046/j.1460-9568.2002.02147.x.
36. H. Burton, A. Z. Snyder, J. B. Diamond, M. E. Raichle, Adaptive changes in early and late blind: A fMRI study of verb generation to heard nouns. Journal of Neurophysiology 88, 3359–3371 (2002).
37. S. Dehaene, L. Cohen, The unique role of the visual word form area in reading. Trends in Cognitive Sciences 15, 254–262 (2011).

38. L. Cohen, S. Dehaene, Specialization within the ventral stream: The case for the visual word form area. NeuroImage 22, 466–476 (2004).
39. M. Behrmann, D. C. Plaut, Distributed circuits, not circumscribed centers, mediate visual recognition. Trends in Cognitive Sciences 17, 210–219 (2013).
40. F. Bouhali, et al., Anatomical connections of the visual word form area. Journal of Neuroscience 34, 15402–15414 (2014).
41. J. D. Yeatman, A. M. Rauschecker, B. A. Wandell, Anatomy of the visual word form area: adjacent cortical circuits and long-range white matter connections. 71, 233–236 (2013).
42. I. M. Schepers, J. F. Hipp, T. R. Schneider, B. Röder, A. K. Engel, Functionally specific oscillatory activity correlates between visual and auditory cortex in the blind. Brain 135, 922–934 (2012).
43. P. Hagoort, The neurobiology of language beyond single-word processing. Science, 55–58 (2019).
44. D. O. Hebb, The Organization of Behavior; A Neuropsychological Theory. The American Journal of Psychology 63, 633 (1950).
45. A. Batardière, et al., Early specification of the hierarchical organization of visual cortical areas in the macaque monkey. Cerebral Cortex 12, 453–465 (2002).
46. S. Rohlf, B. Habets, M. von Frieling, B. Röder, Infants are superior in implicit crossmodal learning and use other learning mechanisms than adults. eLife 6, 1–23 (2017).
47. M. C. Murphy, et al., Top-down influence on the visual cortex of the blind during sensory substitution. NeuroImage 125, 932–940 (2016).
48. D. Bavelier, D. M. Levi, R. W. Li, Y. Dan, T. K. Hensch, Removing brakes on adult brain plasticity: From molecular to behavioral interventions. Journal of Neuroscience 30, 14964–14971 (2010).
49. A. S. Keuroghlian, E. I. Knudsen, Adaptive auditory plasticity in developing and adult animals. Progress in Neurobiology 82, 109–121 (2007).
50. L. Magrou, et al., How areal specification shapes the local and interareal circuits in a macaque model of congenital blindness. Cerebral Cortex 28, 3017–3034 (2018).
51. C. J. Price, J. T. Devlin, The Interactive Account of ventral occipitotemporal contributions to reading. Trends in Cognitive Sciences 15, 246–253 (2011).
52. K. Friston, Learning and inference in the brain. Neural Networks 16, 1325–1352 (2003).
53. K. Friston, The free-energy principle: A unified brain theory? Nature Reviews Neuroscience 11, 127–138 (2010).
54. K. Ren, S. Liu, M. Lin, Y. Wang, Q. M. Zhang, A compact electroactive polymer actuator suitable for refreshable Braille display. Sensors and Actuators, A: Physical 143, 335–342 (2008).
55. T. Völkel, G. Weber, U. Baumann, Tactile graphics revised: The novel BrailleDis 9000 pin-matrix device with multitouch input. Lecture Notes in Computer Science (including subseries Lecture Notes in Artificial Intelligence and Lecture Notes in Bioinformatics) 5105 LNCS, 835–842 (2008).
56. Y. Jiao, X. Lu, Y. Xu, A graphical tactile display for the visually impaired. 2018 (2018).

57. R. W. Cox, AFNI: Software for analysis and visualization of functional magnetic resonance neuroimages. Computers and Biomedical Research 29, 162–173 (1996).
58. C. Destrieux, B. Fischl, A. Dale, E. Halgren, Automatic parcellation of human cortical gyri and sulci using standard anatomical nomenclature. NeuroImage 53, 1–15 (2010).
59. S. Abboud, L. Cohen, Distinctive Interaction Between Cognitive Networks and the Visual Cortex in Early Blind Individuals. Cerebral cortex (New York, N.Y.□: 1991) 29, 4725–4742 (2019).
60. C. G. Yan, X. Di Wang, X. N. Zuo, Y. F. Zang, DPABI: Data Processing & Analysis for (Resting-State) Brain Imaging. Neuroinformatics 14, 339–351 (2016).
61. X. Wang, A. Caramazza, M. V. Peelen, Z. Han, Y. Bi, Reading without speech sounds: VWFA and its connectivity in the congenitally deaf. Cerebral Cortex (2015) https:/doi.org/10.1093/cercor/bhu044.
62. C. G. Yan, et al., A comprehensive assessment of regional variation in the impact of head micromovements on functional connectomics. NeuroImage 76, 183–201 (2013).
63. A. M. Winkler, G. R. Ridgway, G. Douaud, T. E. Nichols, S. M. Smith, Faster permutation inference in brain imaging. NeuroImage 141, 502–516 (2016).
64. X. Chen, B. Lu, C. G. Yan, Reproducibility of R-fMRI metrics on the impact of different strategies for multiple comparison correction and sample sizes. Human Brain Mapping 39, 300–318 (2018).
65. W. H. Jung, S. Lee, C. Lerman, J. W. Kable, Amygdala Functional and Structural Connectivity Predicts Individual Risk Tolerance. Neuron 98, 394-404.e4 (2018).
66. K. J. Friston, L. Harrison, W. Penny, Dynamic causal modelling. NeuroImage 19, 1273–1302 (2003).
67. P. Zeidman, et al., A guide to group effective connectivity analysis, part 1: First level analysis with DCM for fMRI. NeuroImage 200, 174–190 (2019).
68. W. D. Penny, et al., Comparing families of dynamic causal models. PLoS Computational Biology 6 (2010).
69. M. L. Seghier, G. Josse, A. P. Leff, C. J. Price, Lateralization is predicted by reduced coupling from the left to right prefrontal cortex during semantic decisions on written words. Cerebral Cortex 21, 1519–1531 (2011).

Figures and Tables

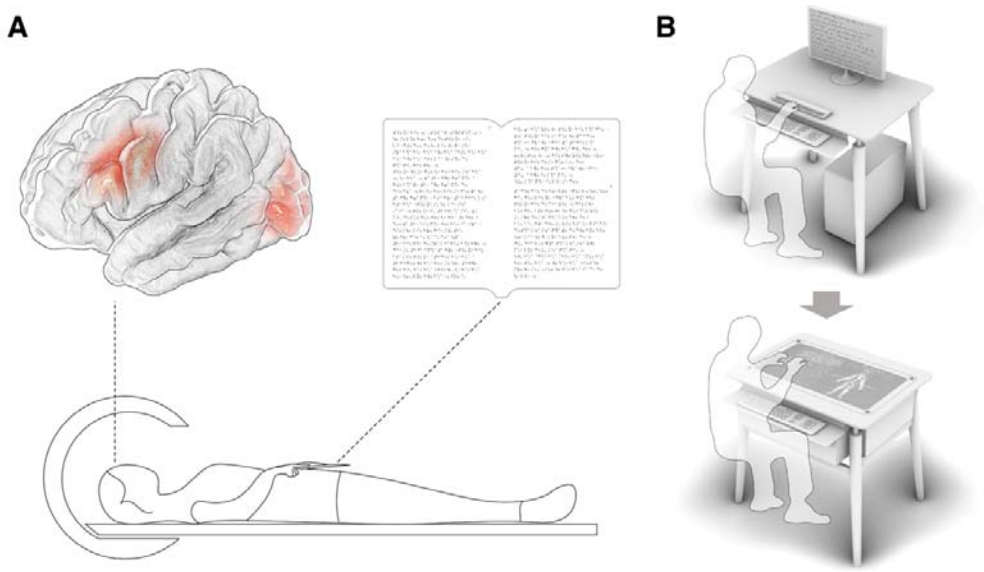

Figure 1. Schematic overview of the study and natural Braille reading devices for blind people. (A) Both resting-state signals and dynamic task-related fMRI data were assessed. The resting-state functional connectivity of two visual brain regions (V1 and LOC), especially with the frontal cortex, was compared between acquired blindness and sighted groups respectively. The task fMRI paradigm was designed to simulate real-life Braille reading using large-format, natural Braille texts. (B) Inspiration for the change from a traditional Braille display (upper panel) containing limited, single-line Braille words to the design of a natural Braille reading device (lower panel) enabling continuous Braille article display for blind individuals.

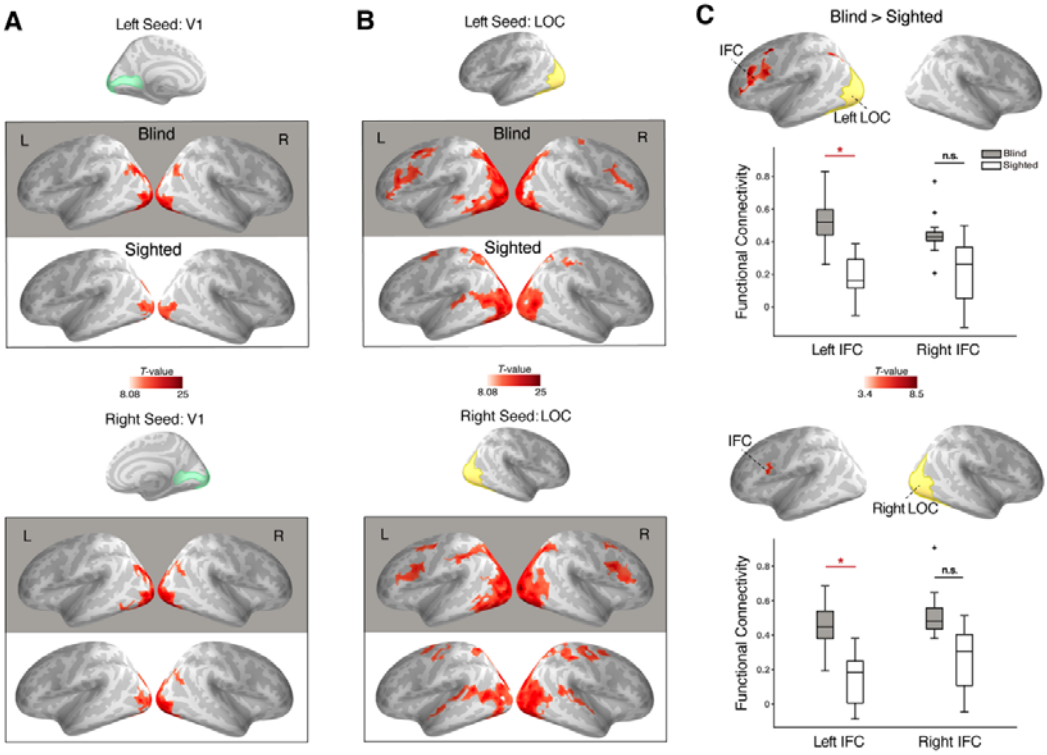

Figure 2. Functional connectivity patterns for the primary 'visual' cortex (V1) and lateral occipital cortex (LOC). (A) Maps show vertices with significant positive connectivity with the left and right V1 seeds respectively (vertexwise $P < 10^{-6}$, uncorrected, cluster size > 100 mm) in the blind group and sighted group. The functional connectivity pattern in the blind group was similar to that in the sighted group, and no significant differences were found between the two. (B) Maps show vertices with significantly positive connectivity with the left and right LOC seeds respectively (vertexwise $P < 10^{-6}$, uncorrected, cluster size > 100 mm) in the blind group and sighted group. (C) Differences in functional connectivity patterns for LOC in the blind group versus the sighted group. Significant vertices were corrected for multiple comparisons using permutation testing with threshold-free cluster enhancement ($P < 0.025$, corrected for each hemisphere, cluster size > 15 mm). Box plot of connectivity strengths (Fisher r-to-z-transformed) between the left (or right) LOC and the left (or right) IFC cluster (in B) for the two groups. Horizontal bars represent the medians, and asterisks indicate significance. V1, primary visual cortex (light green); LOC, lateral occipital cortex (light yellow); IFC, inferior frontal cortex. Blind, dark colour; Sighted, light colour. L left hemisphere, R right hemisphere. *$P < 0.025$ for each hemisphere, corrected. n.s. non-significant.

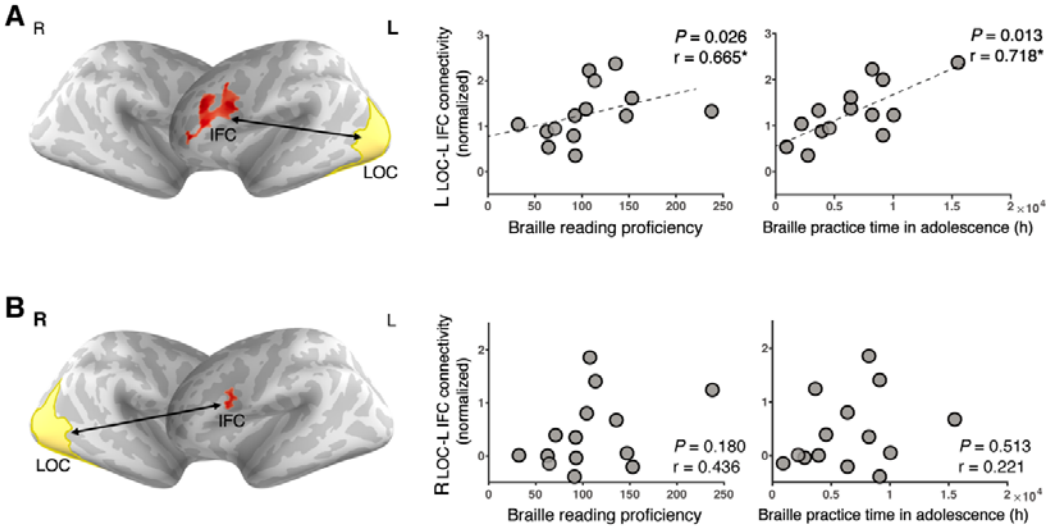

Figure 3. Left LOC-IFC functional coupling predicts Braille reading proficiency and is positively correlated with Braille reading practice time in adolescence. (A) ROIs and their connection. Plots of strong and positive correlation between individual strengths of left LOC-IFC connectivity and Braille reading proficiency (left panel) and Braille reading practice time in adolescence (right panel). (B) ROIs and their connection. The plots illustrate that the functional connectivity between the right LOC and left IFC in the blind group had no significant correlation with either Braille reading proficiency (left panel) or Braille reading practice time in adolescence (right panel). L left hemisphere, R right hemisphere.

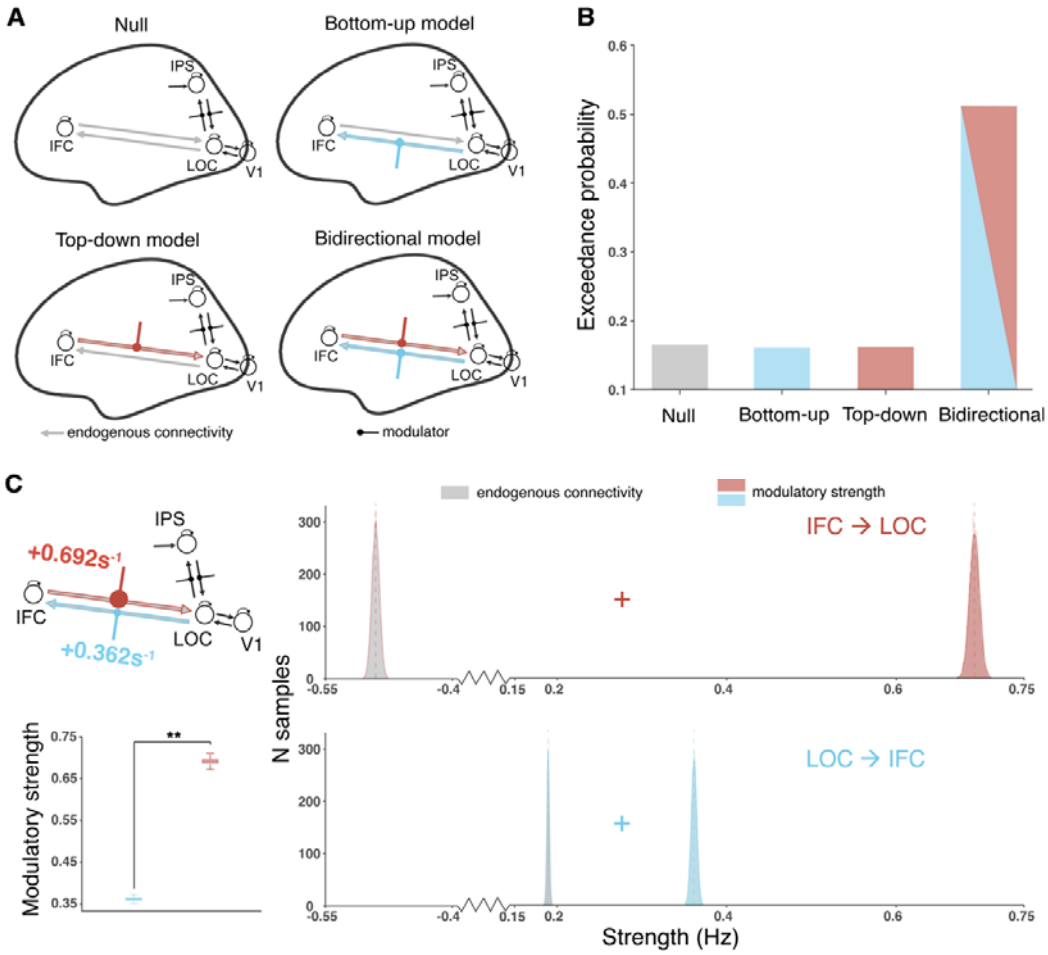

Figure 4. DCM analyses of left LOC-IFC effective connectivity for natural Braille reading. (A) Model space specified by adding task modulation to different directions of the left LOC-IFC connection, resulting in 4 competing models. (B) Exceedance probability for the DCM models, corresponding to the model labels in (A). (C) Illustration of the Bayesian model averaging (BMA) result of the winning bidirectional model for the blind group (all significant at a posterior probability threshold of 0.99). Modulators added to the LOC-IFC connection are coded in the size of the filled circles, representing their effect size (left panel). The modulatory strength of Braille reading on the IFC → LOC connection was significantly higher than that on the LOC → IFC connection ($P < 0.001$). For each parameter (endogenous or modulatory) of the top-down IFC → LOC connection and the bottom-up LOC → IFC connection, the distribution of the 10,000 samples of the posterior densities is provided respectively. Endogenous connectivity: gray; modulatory strength: red for IFC → LOC connection, cyan for LOC → IFC connection. $^{**}P < 0.001$.

Table 1. Characteristic of blind subjects.

	Sex	Age	Onset Age (years)	Braille reading practice time				Braille Reading Proficiency (words/min)	Cause of Blindness
				Start Age (years)	Childhood (h)	Adolescence (h)	Adulthood (h)		
B1	F	23.54	14.72	9.88	4255.90	8212.50	1769.21	92.41	Glaucoma
B2	M	21.39	4.41	7.68	3153.60	9125.00	2951.03	91.15	Ocular pathology
B3	F	22.54	4.12	9.84	2759.40	2737.50	1193.55	92.85	Unknown
B4	F	22.00	5.41	7.29	7736.18	6387.50	1095.00	104.19	Optic nerve atrophy
B5	M	19.20	12.00	6.88	2802.00	3650.00	83.43	237.85	Retinal detachment
B6	F	20.31	5.41	7.99	2194.50	6387.50	449.43	153.08	Trauma
B7	M	19.73	15.00	15.00	-	2190.00	680.50	32.10	Macular discoloration
B8	M	23.28	11.18	13.93	-	3923.50	-	62.51	Glaucoma
B9	F	23.87	7.00	7.52	1637.00	912.50	205.29	64.33	Optic nerve atrophy
B10	M	20.35	11.00	6.99	10065.00	10037.50	339.86	147.04	Unknown
B11	M	24.44	9.00	11.08	1002.00	8212.50	220.14	107.57	Ocular pathology
B12	F	18.68	6.00	7.13	6221.43	9125.00	489.10	113.50	Trauma
B13	F	23.46	8.00	6.91	8360.33	15512.50	2917.39	135.68	Glaucoma
B14	M	24.14	10.00	7.28	4307.00	4562.50	848.89	71.07	Glaucoma